Natural Products (1)

DOI: 10.1002/anie.200902028

The True Structures of the Vannusals, Part 1: Initial Forays into Suspected Structures and Intelligence Gathering**

K. C. Nicolaou, Hongjun Zhang, and Adrian Ortiz*

Isolated from the tropical interstitial ciliate *Euplotes vannus* strains Si121 and BUN3, vannusals A and B were assigned structures **1** and **2**, respectively (Figure 1).[1,2] These novel and challenging molecular architectures have fascinated scientists since their disclosure in 1999, and stood defiant to chemical synthesis until 2008, when we reported the first total synthesis of the originally assigned structure of vannusal B (**2**) and proved it to be wrong.[3] The puzzle of the correct structure of vannusal B was complicated by the scarcity of the natural product and its unprecedented carbon framework, thus leaving the challenge of its solution to chemical synthesis. In this and the following communication,[4] we report our investigations that led to the total synthesis of several suspected stereoisomers of this molecule and the eventual elucidation of its true structure (and that of its sibling, vannusal A) through its total synthesis.

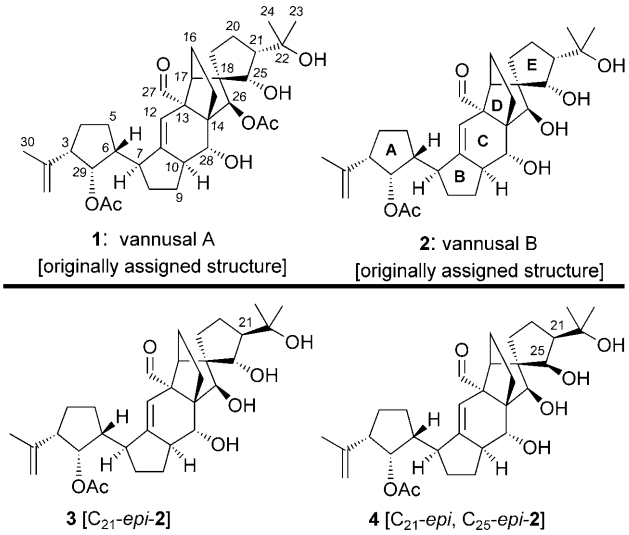

Figure 1. Originally assigned structures of vannusals A (**1**) and B (**2**) and initially targeted stereoisomers **3** [C_{21}-*epi*-**2**] and **4** [C_{21}-*epi*, C_{25}-*epi*-**2**].

Based on the interplay between total synthesis and NMR spectroscopy, the journey to the true structure of vannusal B was long and arduous. It became urgent and was initiated immediately upon completion of the total synthesis of its originally assigned structure (**2**).[3] In the following description, we unravel the logical evolution of events that led to the emergence of useful intelligence that allowed the eventual solution of the vannusal conundrum. Thus, upon comparison of the NMR spectroscopic data of natural vannusal B and synthetic **2**, it became apparent that the most striking differences were located in the "northeastern" region of the molecule, particularly around rings D and E. Strong NMR spectroscopic evidence (see Figure 2) indicated that stereocenters C_{26} (*w*-coupling, $JH_{26,15left} = 1.6$ Hz; NOE, H_{26}/H_{27}) and C_{18} (NOE, H_{25}/H_{16}) were likely to be correct, thus leaving C_{25} and C_{21} as the most logical positions to start our structural modifications. This narrowed our choice to four diastereomeric structures, one of which (i.e. **2**) we had already synthesized.[3] From the remaining three, we selected the C_{21}-*epi* diastereomer of **2**, structure **3** (Figure 1), as our next target molecule based on a subtle and intriguing observation: inversion of the configuration at C_{21} would bring the "northeastern" domain of vannusal B in line with the proposed biosynthetic hypothesis that postulated dimerization of two identical monomeric units (prevannusal, which is naturally

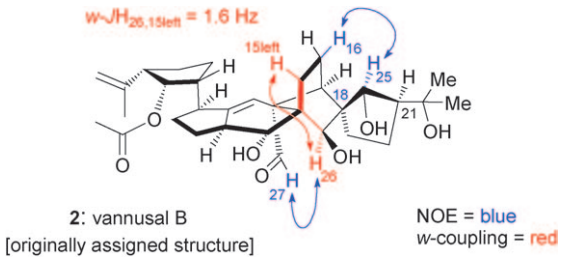

Figure 2. Key ^{1}H NMR coupling constant (*w*-$JH_{26,15left} = 1.6$ Hz) and NOE interaction exhibited by both the originally assigned structure (synthetic, **2**) and natural vannusal B.

[*] Prof. Dr. K. C. Nicolaou, Dr. H. Zhang, A. Ortiz
Department of Chemistry and
The Skaggs Institute for Chemical Biology
The Scripps Research Institute
10550 North Torrey Pines Road, La Jolla, CA 92037 (USA)
and
Department of Chemistry and Biochemistry
University of California, San Diego
9500 Gilman Drive, La Jolla, CA 92093 (USA)
Fax: (+1) 858-784-2469
E-mail: kcn@scripps.edu

[**] We thank Prof. Graziano Guella for samples and NMR spectra of vannusals A and B, and for helpful discussions. We also thank Dr. D. H. Huang, Dr. G. Siuzdak, and Dr. R. Chadha for NMR spectroscopic, mass spectroscopic, and X-ray crystallographic assistance, respectively. Financial support for this work was provided by the NSF (fellowship to A.O.), the Skaggs Institute for Research, and a grant from the National Institutes of Health (USA). We thank Prof. Y. Iwabuchi and Nissan Chemical Industries, Ltd. for generous gifts of AZADO and 1-Me-AZADO catalysts.

Supporting information for this article is available on the WWW under http://dx.doi.org/10.1002/anie.200902028.

occurring)[2] as the biosynthetic precursors to vannusals A and B.

The strategy for the total synthesis of the targeted vannusal B diastereomer **3** relied on the retrosynthetic analysis outlined in Figure 3. Thus, based on our experience

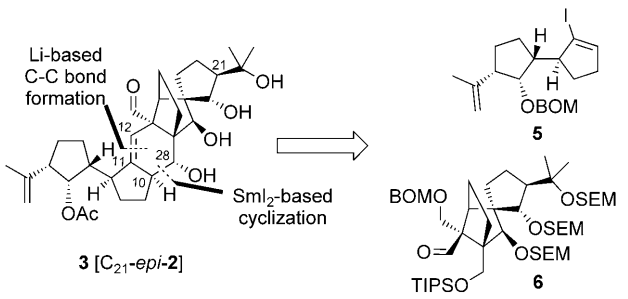

Figure 3. Retrosynthetic analysis of vannusal B stereoisomer **3** [C_{21}-*epi*-**2**]. BOM = benzyloxymethyl, SEM = trimethylsilylethoxymethyl, TIPS = triisopropylsilyl.

in the total synthesis of the originally assigned structure of vannusal B (**2**),[3] we dissected structure **3** at the indicated bonds through a) a lithium-mediated coupling reaction (C_{11}-C_{12}, originally as a C–C bond and eventually as a C=C bond), and b) a SmI_2-based[5] cyclization (C_{10}-C_{28} bond). Accompanied by appropriate functional group modifications, these disconnections revealed vinyl iodide **5** and aldehyde **6** as potential key building blocks for the proposed construction.

With vinyl iodide (−)-**5** already in hand in its enantiopure form,[3] we proceeded to devise a synthesis for racemic aldehyde **6**, the other required fragment for the construction of structure **3**. This objective demanded different chemistry from that employed in the construction of its C_{21}-*epi* counterpart[3] used to synthesize the originally assigned vannusal B structure (**2**). Thus, and as shown in Scheme 1, epoxide **9** was synthesized through vanadium-catalyzed epoxidation [*t*BuOOH, $VO(acac)_2$ (cat.), 90% yield] of homoallylic alcohol **8**, prepared from racemic **7**[3] by treatment with Martin's sulfurane (87% yield). Epoxide **9** was formed as a single diastereomer through the exquisite stereocontrol exerted by the free homoallylic hydroxy group within substrate **8**. The subsequent task of installing the intended nitrile moiety, through the use of the Nagata reagent (Et_2AlCN), however, required protection of this hydroxy group as an acetate group (Ac_2O, Et_3N, DMAP, 90% yield).[6] Upon exposure to Et_2AlCN, the latter compound afforded the targeted *trans* hydroxy nitrile **11**, as expected, in 81% yield. Removal of the acetate group from **11** (K_2CO_3, MeOH) furnished the required dihydroxy nitrile **12**, in quantitative yield. The structure of **12** was secured unambiguously by X-ray crystallographic analysis[7] (see ORTEP drawing, Scheme 1) of its crystalline acetonide derivative **13** (m.p. 87–88 °C, hexanes), which was prepared by exposure of **12** to 2,2-dimethoxypropane in the presence of PPTS (cat.; 89% yield).

The elaboration of dihydroxy nitrile **12** to aldehyde **6** is summarized in Scheme 2. Thus, protection of the hydroxy groups of **12** with SEM moieties (SEMCl, iPr_2NEt, 90% yield) led to bis-SEM derivative **14**, which was then converted into tertiary alcohol **15** through a four-step sequence (reduction with DIBAL-H, MeMgBr addition, oxidation with NMO-TPAP (cat.), and MeMgBr addition to give 72% yield over 4 steps). Capping the newly generated tertiary hydroxy group within **15** required more forcing reaction conditions (SEMCl, KHMDS, THF, −78→25 °C, 92% yield), and led to the expected tri-SEM derivative **16**. The remaining steps to the desired aldehyde **6** followed our previously developed strategy[3] which required initial ozonolysis of **16** (89% yield) and subsequent enolization/*O*-alkylation of the resulting aldehyde (KH, allyl chloride) to afford allyl enol ether **17** (91% yield). Heating of the latter under microwave (MW) conditions (200 °C) effected the desired Claisen rearrangement, and reduction with $NaBH_4$ converted the resulting aldehyde into the primary alcohol **18** (91% yield over 2 steps). Subsequent protection of the primary hydroxy group within the latter (BOMCl, iPr_2NEt, nBu_4NI) and ozonolysis (O_3; Ph_3P) led to **19** (92% yield over 2 steps),

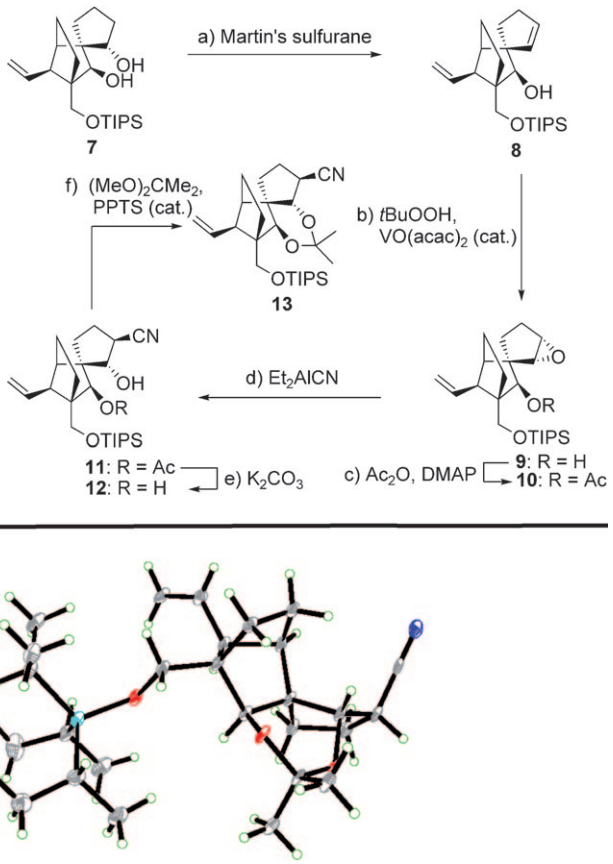

Scheme 1. Construction of nitrile **12** (top) and X-ray crystal structure of **13** (bottom; ORTEP: thermal ellipsoids are shown at 30% probability). Reagents and conditions: a) Martin's sulfurane (1.1 equiv), Et_3N (10 equiv), CH_2Cl_2, 25 °C, 5 h, 87%; b) *t*BuOOH (3.0 equiv), $VO(acac)_2$ (0.2 equiv), benzene, 25 °C, 6 h, 90%; c) Ac_2O (10 equiv), Et_3N (30 equiv), DMAP (1.0 equiv), CH_2Cl_2, 4 h, 25 °C, 90%; d) Et_2AlCN (10 equiv), toluene, −78→−20 °C, 19 h, 81%; e) K_2CO_3 (1.0 equiv), MeOH, 25 °C, 2 h, quant.; f) DMF/2,2-dimethoxypropane (1:1), PPTS (1.0 equiv), 24 h, 89%. acac = acetylacetonate, DMAP = 4-dimethylaminopyridine, DMF = *N*,*N*-dimethylformamide, PPTS = pyridinium 4-toluenesulfonate.

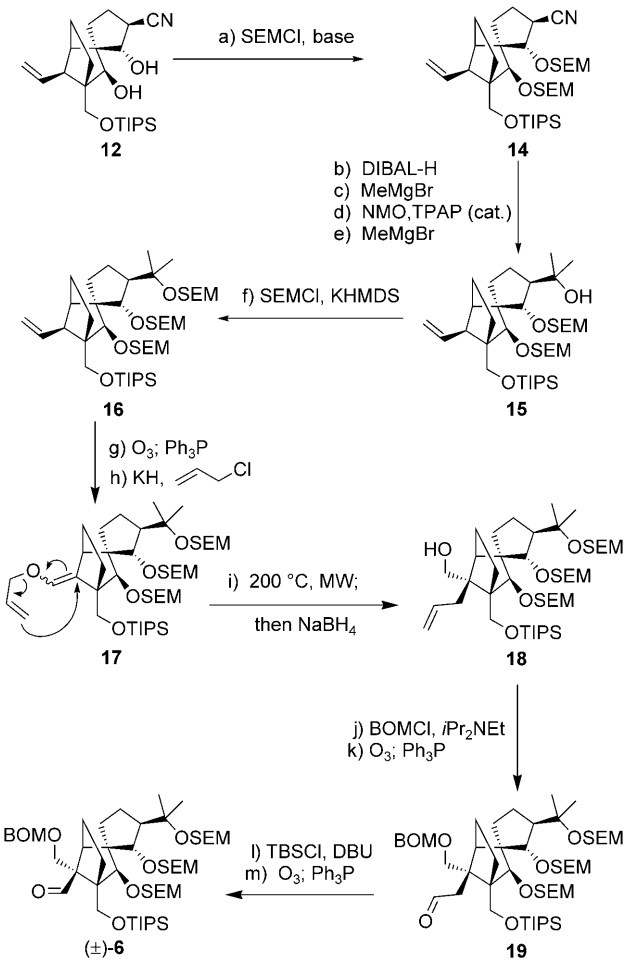

Scheme 2. Construction of aldehyde (±)-**6**. Reagents and conditions: a) SEMCl (10 equiv), iPr$_2$NEt (30 equiv), CH_2Cl_2, 50 °C, 48 h, 90%; b) DIBAL-H (1.1 equiv), toluene, −78→30 °C, 1 h; then 0.1 M HCl, 25 °C, 20 min; c) MeMgBr (10 equiv), THF, 0 °C, 30 min; d) NMO (2.0 equiv), TPAP (0.05 equiv), CH_2Cl_2/CH_3CN (7:1), 25 °C, 3 h; e) MeMgBr (10 equiv), THF, −10 °C, 20 min, 72% over four steps; f) KHMDS (2.0 equiv), SEMCl (5.0 equiv), Et_3N (10 equiv), −78→25 °C, 1 h, 92%; g) O_3, py (1.0 equiv), CH_2Cl_2/MeOH (1:1), −78 °C; then Ph_3P (5.0 equiv), −78→25 °C, 1 h, 89%; h) KH (10 equiv), allyl chloride (30 equiv), HMPA (10 equiv), DME, 25 °C, 12 h, 91%; i) iPr$_2$NEt (1.0 equiv), o-dichlorobenzene, 200 °C (MW), 20 min; then $NaBH_4$ (10 equiv), MeOH, 1 h, 25 °C, 91% over two steps; j) BOMCl (10 equiv), iPr$_2$NEt (30 equiv), nBu$_4$NI (1.0 equiv), CH_2Cl_2, 50 °C 12 h; k) O_3, py (1.0 equiv), CH_2Cl_2/MeOH (1:1), −78 °C; then Ph_3P (5.0 equiv), −78→25 °C, 1 h, 92% over two steps; l) TBSCl (10 equiv), DBU (20 equiv), CH_2Cl_2, 25 °C, 48 h; m) O_3, py (1.0 equiv), CH_2Cl_2/MeOH (1:1), −78 °C; then Ph_3P (5.0 equiv), −78→25 °C, 1 h, 92% over two steps. DBU = 1,8-diazoicyclo[5.4.0]undec-7-ene, DIBAL-H = diisobutylaluminum hydride, DME = 1,2-dimethoxyethane, HMDS = hexamethyldisilazane, HMPA = hexamethylphosphoramide, MW = microwave, NMO = 4-methylmorpholine *N*-oxide, py = pyridine, TBS = *tert*-butyldimethylsilyl, THF = tetrahydrofuran, TPAP = tetra-*n*-propylammonium perruthenate.

which was finally converted into (±)-**6** through formation of the silyl enol ether (DBU, TBSCl) and another ozonolysis (O_3; Ph_3P) to give 92% yield over two steps.

With both key building blocks (−)-**5** and (±)-**6** in hand, we proceeded with their union and further elaboration of the desired diastereomeric coupling product to its final destination, vannusal B structure **3**, as shown in Scheme 3. Lithium–iodide exchange within (−)-**5** (tBuLi, THF, −78→−40 °C) and subsequent addition of (±)-**6** led to two coupling products (ca. 1:1 d.r.), which, after removal of the TIPS group (TBAF, 25 °C), were separated by chromatography to provide **20** (41% yield over 2 steps) and its diastereomer (**d-20**, not shown, 42% yield over 2 steps). Diastereomer **20** was converted into the cyclization precursor aldehyde carbonate **21** through a four-step sequence involving temporary protection of the primary hydroxy group with a TES group (TESCl, imid.), installation of a carbonate moiety at C_{12} ($ClCO_2Me$, Et_3N), removal of the TES group (HF·py/py (1:4), 79% over 3 steps), and oxidation of the regenerated primary alcohol [PhI(OAc)$_2$-AZADO (cat.),[8] 95% yield]. With precursor **21** at hand, we were then in a position to attempt the crucial SmI_2-induced ring-closure reaction that would forge the entire carbon skeleton of our target molecule, a process whose efficiency and stereochemical outcome we found to be dependent on the nature of the protecting groups residing on the C_{26}, C_{25}, and C_{22} oxygen residues, as well as the relative configuration of the "southwestern" and "northeastern" domains of the molecule (i.e. **20** vs **d-20**). In this instance, the SEM groups at these positions in precursor **21** proved cooperative by facilitating its intended cyclization (SmI_2, HMPA, THF, −20→25 °C) to afford two diastereomers that were separated by chromatography (**22β**, 33% yield and **22α**, 21% yield).[9] Both diastereomers could be easily converted into the same conjugated diene **23** through previously developed procedures[3] as a prelude to correcting their configuration at C_{10} and/or C_{28}. Treatment of **22α** with $POCl_3$ and pyridine led to the formation of **23** in 72% yield, while conversion of **22β** into **23** proceeded through xanthate formation (NaH, CS_2; MeI) and Chugaev *syn*-elimination (MW heating, 185 °C, 86% yield over 2 steps). Conjugated diene **23** was transformed regio- and stereoselectively into intermediate **24**, which possesses the inverted and desired configuration at C_{10} and C_{28}, by sequential hydroboration/oxidation ($ThexBH_2$; BH_3·THF; H_2O_2, 70% yield) and phenylselenenylation/*syn* elimination (o-$NO_2C_6H_4SeCN$, nBu$_3$P; H_2O_2, 68% overall yield). The final drive from **24** to vannusal B structure **3** proceeded through intermediate **25** and required installment of a TES group at C_{28} (TESCl, KHMDS, 89% yield), removal of the BOM groups (LiDBB, 83% yield), selective oxidation of the primary alcohol over the secondary [PhI(OAc)$_2$, 1-Me-AZADO (cat.)],[8] acetylation (Ac_2O, DMAP, 87% yield over 2 steps), and, finally, aqueous HF-induced global deprotection (aq HF/THF (1:3), 77% yield). The AZADO and 1-Me-AZADO catalysts[8] (see structures, Scheme 3) proved to be superior to TEMPO (2,2,6,6-teramethyl-1-piperidinyloxy, free radical) in these studies, and were subsequently employed with success in several other sequences instead of TEMPO. Although consistent with its structure, the NMR spectroscopic data of synthetic vannusal B structure **3** did not match those reported for the natural product, thereby sending us back to the drawing board to contemplate our next move. Disappointing as they were, these data, however, pointed to a new line of investigation. Specifically, the rather large coupling constant

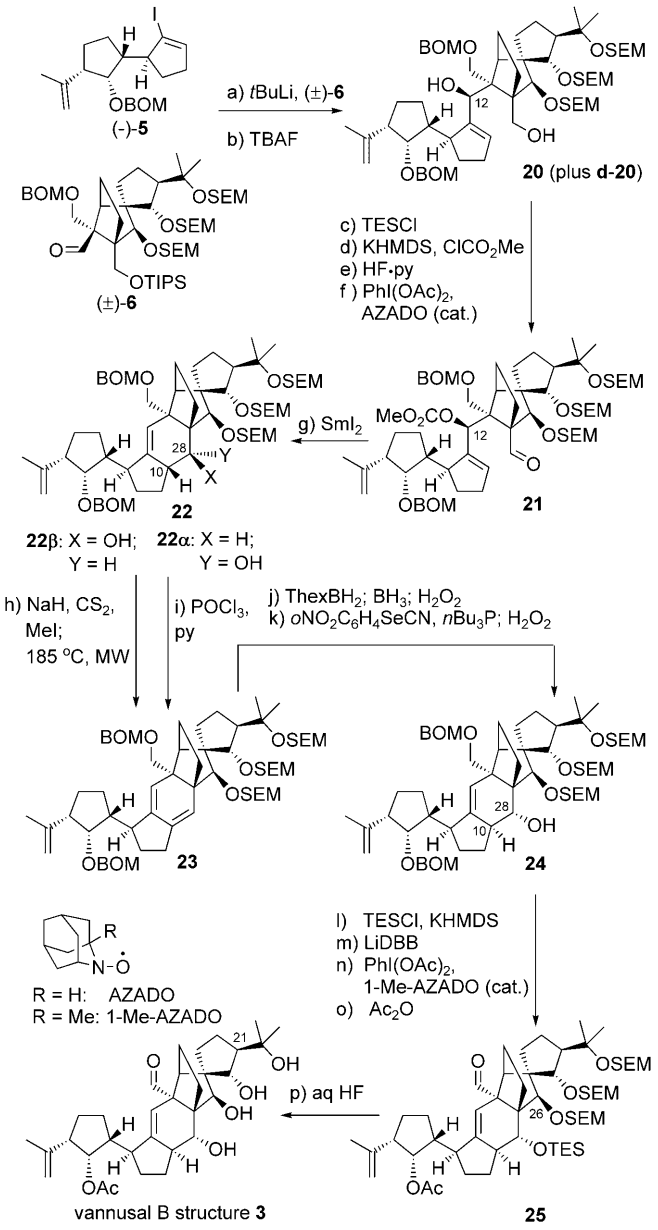

Scheme 3. Synthesis of vannusal B structure **3** [C_{21}-*epi*-**2**]. Reagents and conditions: a) (−)-**5** (1.3 equiv), *t*BuLi (2.5 equiv), THF, −78→−40 °C, 50 min; then (±)-**6** (1.0 equiv), −40→0 °C, 20 min; b) TBAF (2.0 equiv), THF, 25 °C, 6 h, **20**, 41 % over two steps, **d-20**, 42 % over two steps; c) TESCl (2.0 equiv), imid (10 equiv), CH_2Cl_2, 25 °C, 5 h; d) KHMDS (5.0 equiv), $ClCO_2Me$ (10.0 equiv), Et_3N (10 equiv), THF, −78→25 °C, 1 h; e) HF·py/py (1:4), 0→25 °C, 12 h, 79 % over three steps; f) $PhI(OAc)_2$ (2.0 equiv), AZADO (0.1 equiv), CH_2Cl_2, 25 °C, 24 h, 95 %; g) SmI_2 (0.1 M in THF, 4.0 equiv), HMPA (12 equiv), THF, −20→25 °C, 3.5 h, **22β**, 33 %, **22α**, 21 %; h) NaH (15 equiv), CS_2 (30 equiv), THF, 0→25 °C, 30 min; then MeI (45 equiv), 25 °C, 24 h; then MW heating, 185 °C), *o*-dichlorobenzene, 15 min, 86 % over two steps; i) $POCl_3$, py, 72 %; j) $ThexBH_2$ (5.0 equiv), THF, −10→25 °C, 0.5 h; then BH_3·THF (15 equiv), 25 °C, 1 h; then 30 % H_2O_2/3 N NaOH (1:1 d.r.), 0→45 °C, 1 h; 70 %; k) $oNO_2C_6H_4SeCN$ (3.0 equiv), nBu_3P (6.0 equiv), py (9.0 equiv), THF, 25 °C; then 30 % H_2O_2, 0→45 °C, 68 %; l) KHMDS (6.0 equiv), TESCl (4.0 equiv), Et_3N (8.0 equiv), THF, −50→25 °C, 30 min, 89 %; m) LiDBB (excess), THF, −78→-50 °C, 1 h, 83 %; n) $PhI(OAc)_2$ (2.0 equiv), 1-Me-AZADO (0.2 equiv), CH_2Cl_2, 25 °C, 22 h; o) Ac_2O (30 equiv), Et_3N (90 equiv), DMAP (2.0 equiv), CH_2Cl_2, 25 °C, 36 h, 87 % over two steps; p) 48 % aq HF/THF (1:3), 25 °C, 7 h, 77 %. imid = imidazole, LiDBB = lithium di-*tert*-butylbiphenyl, TBAF = tetra-*n*-butylammonium fluoride, TES = triethylsilyl, Thex = thexyl.

between H_{25} and H_{21} ($J_{H25,21}$ = 8.5 Hz, see Figure 4) exhibited in the ^{1}H NMR spectrum of **3** (a C_{25}/C_{21} *trans* structure) seemed to suggest that the true structure of vannusal B (exhibiting $J_{H25,21}$ = 1.6 Hz) possessed a C_{25}/C_{21} *cis* arrangement rather than a *trans* relationship.

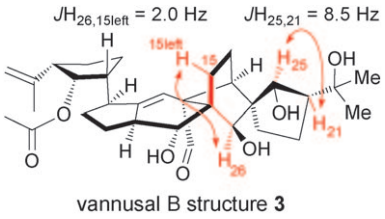

Figure 4. Key ^{1}H NMR coupling constants of vannusal B structure **3** ($J_{H25,21}$ = 8.5 Hz, *w*-$J_{H26,15left}$ = 2.0 Hz).

Having excluded structure **3** [C_{21}-*epi*-**2**] as the true structure of vannusal B, we then moved to our second target, diastereomer **4** [C_{21}-*epi*, C_{25}-*epi*-**2**], which possesses a C_{25}/C_{21} *cis* relationship, as a possibility for the coveted vannusal B structure. The aldehyde building block **30** required for this construction was synthesized from diketone **26**[3] as summarized in Scheme 4. Thus, generation of the lithium enolate from **26** (LDA, −78→−40 °C) and subsequent addition of acetone led to a diastereomeric mixture of aldol products in which the β stereoisomer predominated (ca. 3:1 d.r.). Protection of the hydroxy group with a TES group (TESOTf, 2,6-lutidine) and subsequent separation by chromatography furnished isomerically pure diketone **27** (66 % yield over 2 steps), which was selectively reduced from the α face with $NaBH_4$ (THF/MeOH (1:1), −10→25 °C) at both carbonyl sites to afford, after removal of the TES group (PPTS, EtOH), triol **28** in 91 % yield. Regioselective formation of an acetonide group within the latter intermediate [$(MeO)_2CMe_2$, PPTS, quantitative yield], and subsequent installation of the SEM group (SEMCl, iPr_2NEt, nBu_4NI, 97 % yield) led to intermediate **29**. The latter was converted into the desired aldehyde, (±)-**30**, by the same route (and in similar yields) as the one described above for the conversion of **16** into (±)-**6** (see Scheme 2), as summarized in Scheme 4.

The total synthesis of vannusal B diastereomeric structure **4** [C_{21}-*epi*, C_{25}-*epi*-**2**] from (−)-**5** and (±)-**30** (see Scheme 4) proceeded through similar intermediates and along the same lines as the route to vannusal B structure **3** [C_{21}-*epi*-**2**] from (−)-**5** and (±)-**6** discussed above (see Scheme 3). Notable differences between the two routes were the higher yield obtained in the SmI_2-mediated ring closure step (74 % yield), which was most likely a consequence of the use of the acetonide moiety at the C_{25}/C_{21} site, and the isolation of only one diastereomer at this stage, corresponding to **22β** (Scheme 3). Again, the NMR spectroscopic data of synthetic structure **4** were disappointing in that they did not match those of the natural vannusal B. However, we

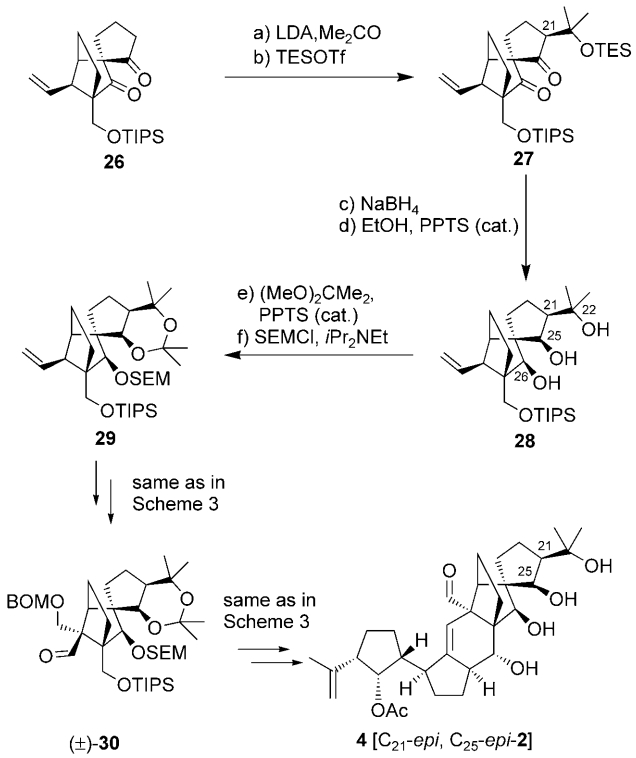

Scheme 4. Synthesis of aldehyde (±)-**30** and vannusal B structure **4**. Reagents and conditions: a) LDA (generated from iPr_2NH (5.0 equiv), *n*BuLi (2.5 M in haxanes, 5.0 equiv)), THF, −78→−40 °C; then acetone (20 equiv), −40→25 °C, 1 h, (3:1 d.r.); b) TESOTf (2.0 equiv), 2,6-lutidine (5.0 equiv), −78→−40 °C, 1 h, 66% over two steps; c) $NaBH_4$ (20 equiv), THF/MeOH (1:1), −10→25 °C, 4 h; d) EtOH, PPTS (0.10 equiv), 25 °C, 2 h, 91% over two steps; e) $(MeO)_2C(Me)_2$/DMF (1:1), PPTS (1.0 equiv), 25 °C, 48 h, quant.; f) SEMCl (5.0 equiv), iPr_2NEt (15 equiv), nBu_4NI (1.0 equiv), CH_2Cl_2, 50 °C, 24 h, 97%. LDA = lithium diisopropylamide.

were encouraged by the ^{1}H NMR spectrum of this structure, which revealed much closer chemical shifts for H_{17} and H_{26} ($\delta H_{17} = 2.50$; $\delta H_{26} = 4.05$ ppm) to those exhibited by the natural product ($\delta H_{17} = 2.48$ ppm; $\delta H_{26} = 3.95$ ppm) than those in the originally assigned structure **2**, whose chemical shifts for these protons were far from close ($\delta H_{17} = 2.25$ ppm; $\delta H_{26} = 4.40$ ppm) to those of the natural product (see Figure 5). Based on these observations, we surmised that the "northeastern" domain (i.e. ring E) of the true structure of vannusal B possessed the configuration shown in structure **4**, which has the *cis* C_{25}/C_{21} stereochemical arrangement (Figure 1). At this point, we turned our attention to the "southwestern" part of the molecule (i.e. ring A) with the aim of making stereochemical changes in that region to define our next targets.

Careful consideration of the reported ^{1}H NMR spectroscopic data of both vannusals A and B led us to believe that the relative configuration at C_6 with respect to C_3, C_{29}, and C_7 of the originally assigned structures of the vannusals (i.e. **1**; see Figure 6a) was correct. This assumption was based on a) the rather large ^{1}H NMR coupling constant between H_6 and H_7 ($JH_{6,7} = 10.0$ Hz), which supported the assigned *trans*-diaxial orientation of these two protons, and b) the observed

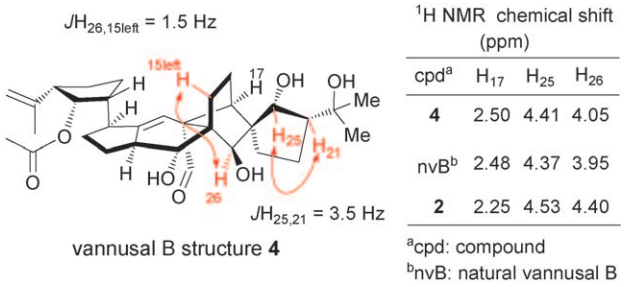

^{1}H NMR chemical shift (ppm)			
cpd[a]	H_{17}	H_{25}	H_{26}
4	2.50	4.41	4.05
nvB[b]	2.48	4.37	3.95
2	2.25	4.53	4.40

[a]cpd: compound
[b]nvB: natural vannusal B

Figure 5. Key ^{1}H NMR coupling constants (w-$JH_{26,\ 15left} = 1.5$ Hz, $JH_{25,\ 21} = 3.5$ Hz) and selected chemical shifts for vannusal B structure **4** and comparisons with those of natural vannusal B (nvB) and its originally assigned structure **2**.

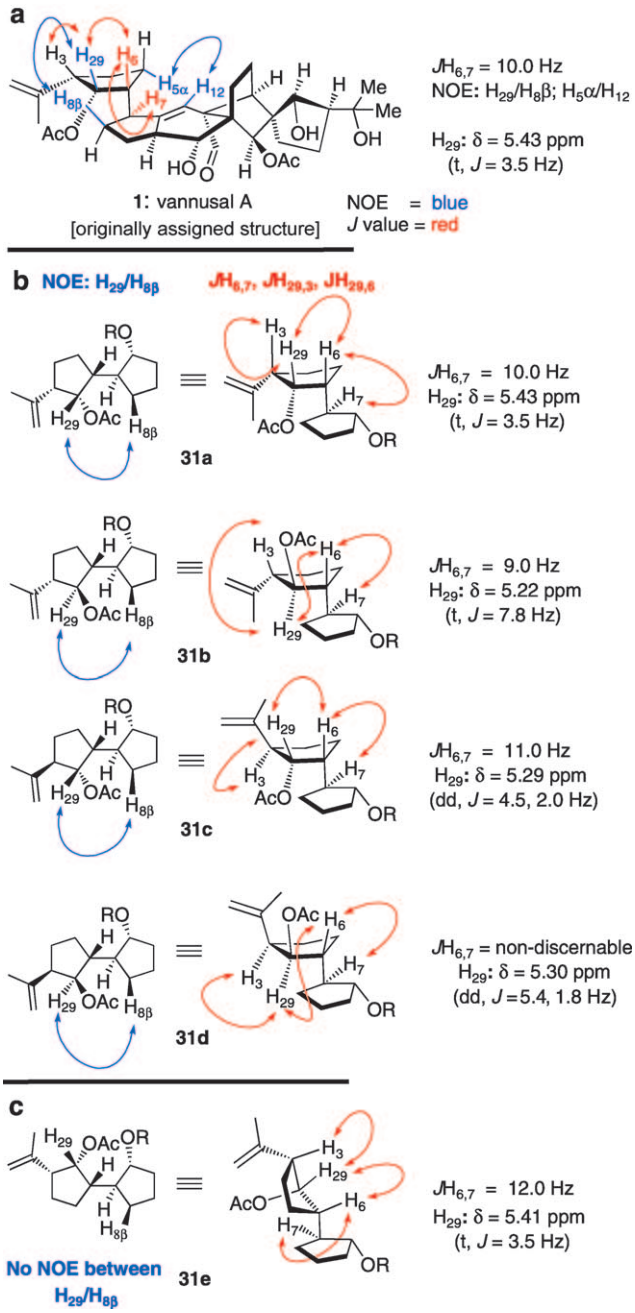

Figure 6. Relevant NOE interactions and coupling constants (J) of AB-ring model compounds **31a**–**31e**. R = TBDPS = *tert*-butyldiphenylsilyl.

NOE interactions between H_{29} and $H_{8\beta}$, and $H_{5\alpha}$ and H_{12} (see Figure 6a). Indeed, the 6-*epi* diastereomer of **2** (not shown) is problematic in that it cannot accommodate these observations as supported by model system **31e**[10] (Figure 6c), which exhibits rather similar ^{1}H NMR coupling constants between H_6 and H_7 ($JH_{6,7} = 12.0$ Hz), H_6 and H_{29} ($JH_{6,29} = 3.5$ Hz), and H_3 and H_{29} ($JH_{3,29} = 3.5$ Hz) as those exhibited by the natural product ($JH_{6,7} = 10.0$ Hz; $JH_{6,29} = 3.5$ Hz; $JH_{3,29} = 3.5$ Hz), but no NOE interaction between H_{29} and either of the two H_8 protons. This conclusion left C_3 and C_{29} as the possible sites of structural misassignment in the original report.[1] To elucidate this point, we synthesized all four possible diastereomers of the model AB-ring system (compounds **31a–31d**;[10] Figure 6b) and compared their NMR spectroscopic data with those of the natural vannusal A. Although all four model systems exhibited the expected NOE interactions between H_{29} and $H_{8\beta}$, their ^{1}H NMR chemical shifts and coupling constants of H_{29} were revealing (**31a**: $\delta = 5.43$ ppm, $JH_{29,3} = 3.5$ Hz, $JH_{29,6} = 3.5$ Hz; **31b**: $\delta = 5.22$ ppm, $JH_{29,3} = 7.8$ Hz, $JH_{29,6} = 7.8$ Hz; **31c**: $\delta = 5.29$ ppm, $JH_{29,3} = 4.5$ Hz, $JH_{29,6} = 2.0$ Hz; **31d**: $\delta = 5.30$ ppm, $JH_{29,3} = 1.8$ Hz, $JH_{29,6} = 5.4$ Hz, see Figure 6b). Indeed, the striking resemblance of the ^{1}H NMR spectroscopic data of model system **31a** (as opposed to the other three) to those reported for the natural vannusal A ($\delta = 5.43$ ppm, $JH_{29,3} = 3.5$ Hz, $JH_{29,6} = 3.5$ Hz) were convincing of the correctness of the originally assigned configurations at C_3, C_{29}, C_6, and C_7 of the molecule. It was through this pathpointing intelligence that we returned to the most "northeastern" ring of the vannusal structure to contemplate the remaining possibilities. In the following communciation, we unravel our next course of action and the events that led to the total synthesis of the true structure of vannusal B, and thereby, the elucidation of its molecular architecture, and that of its sibling, vannusal A.

Received: April 15, 2009
Published online: June 27, 2009

Keywords: natural products · NMR spectroscopy · revised structures · structure elucidation · total synthesis

[1] G. Guella, F. Dini, F. Pietra, *Angew. Chem.* **1999**, *111*, 1217–1220; *Angew. Chem. Int. Ed.* **1999**, *38*, 1134–1136.
[2] G. Guella, E. Callone, G. Di Giuseppe, R. Frassanito, F. P. Frontini, I. Mancini, F. Dini, *Eur. J. Org. Chem.* **2007**, 5226–5234.
[3] K. C. Nicolaou, H. Zhang, A. Ortiz, P. Dagneau, *Angew. Chem.* **2008**, *120*, 8733–8738; *Angew. Chem. Int. Ed.* **2008**, *47*, 8605–8610.
[4] K. C. Nicolaou, et al., *Angew. Chem.* **2009**, DOI: 10.1002/ange.200902029; *Angew. Chem. Int. Ed.* **2009**, DOI: 10.1002/anie.200902029, see the following communication in this issue.
[5] For reviews on samarium diiodide used in organic synthesis, see: a) D. J. Edmonds, D. Johnston, D. J. Procter, *Chem. Rev.* **2004**, *104*, 3371–3403; b) H. B. Kagan, *Tetrahedron* **2003**, *59*, 10351–10372; c) G. A. Molander, C. R. Harris, *Chem. Rev.* **1996**, *96*, 307–308.
[6] Reaction of hydroxy epoxide **9** with Et_2AlCN resulted in the predominant transfer of an Et group to the substrate rather than a CN group: presumably this transfer occurs through initial formation of the -$OAlEt_2$ species (C_{26}) and subsequent intramolecular epoxide activation and delivery of an Et group.
[7] CCDC 726953 (**13**) contains the supplementary crystallographic data for this paper. These data can be obtained free of charge from The Cambridge Crystallographic Data Centre via www.ccdc.cam.ac.uk/data_request/cif.
[8] M. Shibuya, M. Tomizawa, I. Suzuki, Y. Iwabuchi, *J. Am. Chem. Soc.* **2006**, *128*, 8412–8413.
[9] Despite the modest yield, this reaction served us well given the failure of the originally employed C_{25}/C_{26} acetonide, C_{21}-SEM precursor to give any cyclization product under the same reaction conditions.
[10] Details of these syntheses will be reported in the full account of this work, selected physical properties of compounds **31a–31e** are given in the Supporting Information.

